

A design approach to mechanical shock mitigation in optomechanical systems

M. Nefzi¹, F. Wagner², K. Baumann²

¹ Carl Zeiss, Mechanics & Mechatronics Concepts
Rudolf-Eber-Straße 2, 73447 Oberkochen, Germany

² ICS Engineering GmbH
Am Lachengraben 5, 63303 Dreieich, Germany

Abstract

Optomechanical systems are very sensitive to external dynamic excitations, which may occur during operation or in the out-of-operation state. Vibration excitations are characterized by a relatively long duration and a small magnitude as well as randomness, whereas shock excitations have a relatively short duration and large magnitude. Both excitation types should be considered while designing robust optomechanical systems that can withstand the resulting loads. In this work, we focus on excitations occurring in the out-of-operation state. First, we discuss different shock and vibration excitations in time and frequency domains and specify realistic profiles that reflect handling and transport conditions. We also show that simplified optomechanical multi-body models are more adequate to specify the stiffness and damping values for hard stops required to prevent collision between system parts. Hard stops lead to a non-linear system since they exert forces once a predefined range is exceeded. However, we show that, to a certain extent, a linear model can be relied upon at an early stage of the design process to derive design specifications. We then address the modelling of one single hard stop based on measurements. The obtained model can be used to verify whether the real dynamic characteristics of the hard stops help prevent large relative displacements and forces between all optical elements.

1 Introduction

Lithography is a highly developed process step in the production of microchips for modern electronic devices. Its purpose is to create small structures on thin silicon discs, known as wafers. The lithographic projection objective is used to project small structures in a reticle onto a light-resistive coating on the wafer. This step is performed by wafer steppers in which the objective is embedded (see Figure 1a). The latest wafer steppers can resolve structure sizes of 22 nm. These extremely small sizes require exceptionally high accuracies in the lithography objective. Hence, even very small excitations during operation can cause erroneous projections. The same applies to small damages which can result from transport, earthquakes, or poor handling while setting up the machine. This paper will focus on the latter issues which are very decisive, especially during the early stages of the design process (see also [1]).

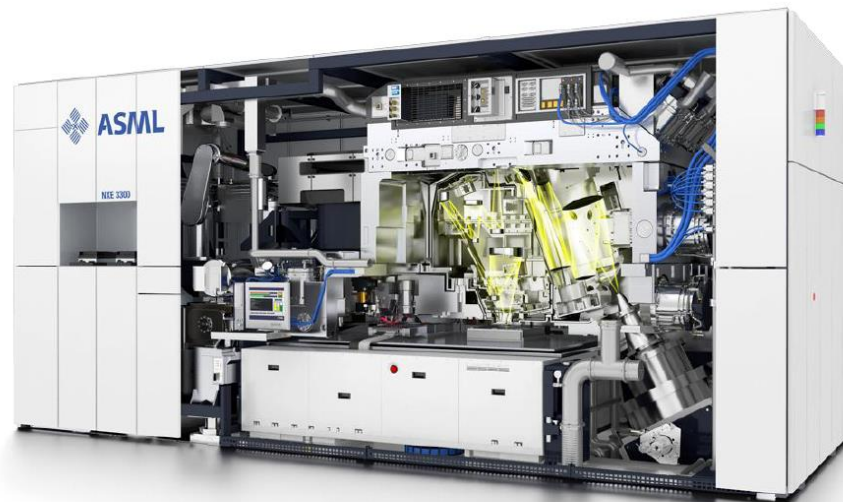


Figure 1a: ASML machine for producing semiconductor devices

Figure 1b depicts a possible approach to mechanical shock mitigation of optomechanical systems which have to withstand tough external excitations during their setting up. Although it is not possible to shed light on each step of this approach within the scope of this work, we will be able to discuss some issues that arise from this approach. Section 2 addresses external shock and vibration excitations that may occur when the machine is out of operation. In Section 3, the non-linear vibration behaviour of a simplified optomechanical system subjected to shock and vibration excitations will be examined and visualized through response curves. Thereafter, we show that it is possible to some extent to rely on a linear model to find out the appropriate characteristics of the hard stops to avoid collisions and large forces. Section 4 addresses the modelling of one single hard stop using measurement curves. The obtained model can be implemented in a more complex 3D multi-body model that allows for the computation of the displacements of all optical elements and the forces in their connections. This, in turn, enables one to check whether the specifications at system level, that is, avoiding collisions and large forces, are met.

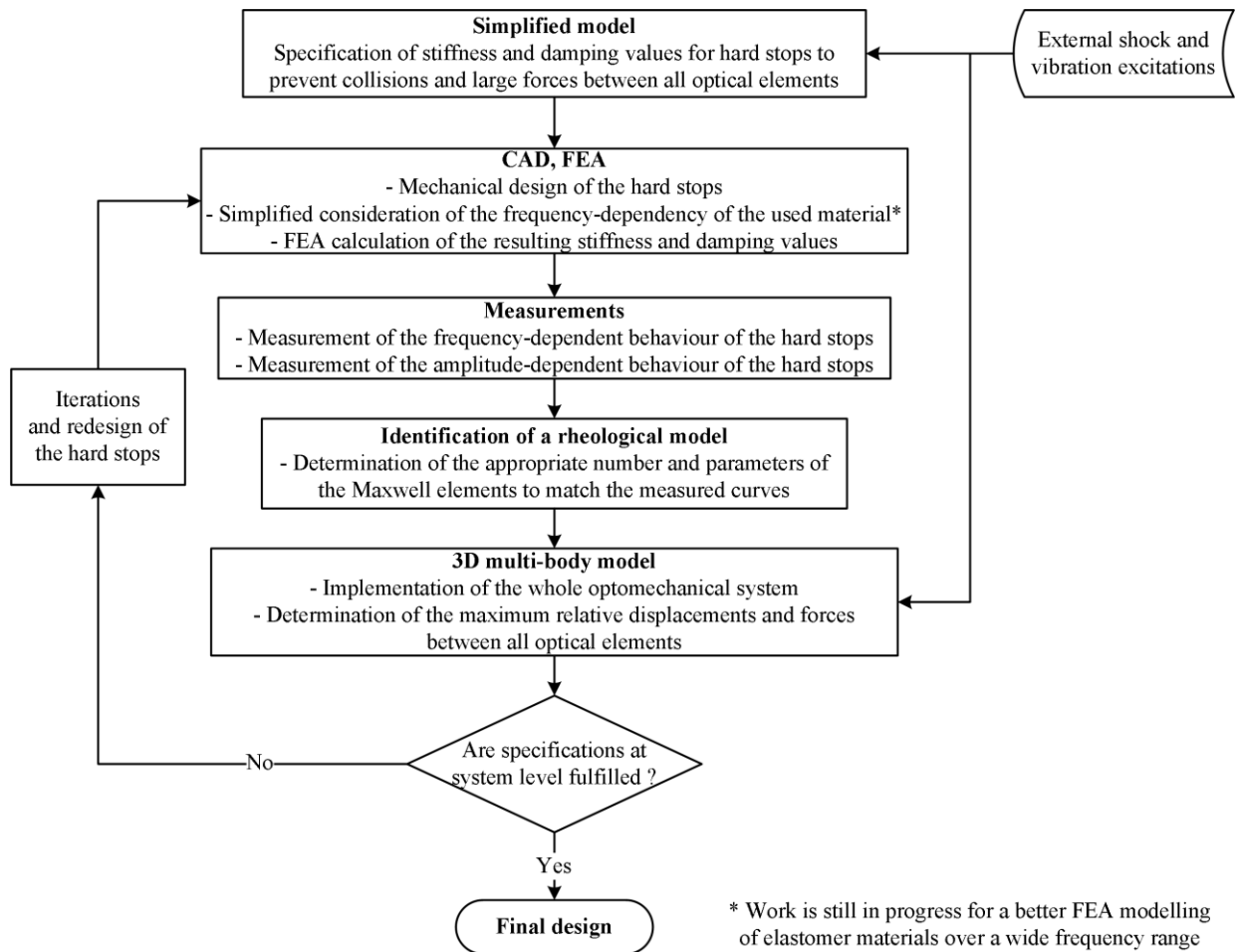


Figure 1b: Design approach to mechanical shock mitigation of optomechanical systems

2 Handling and Transport Conditions

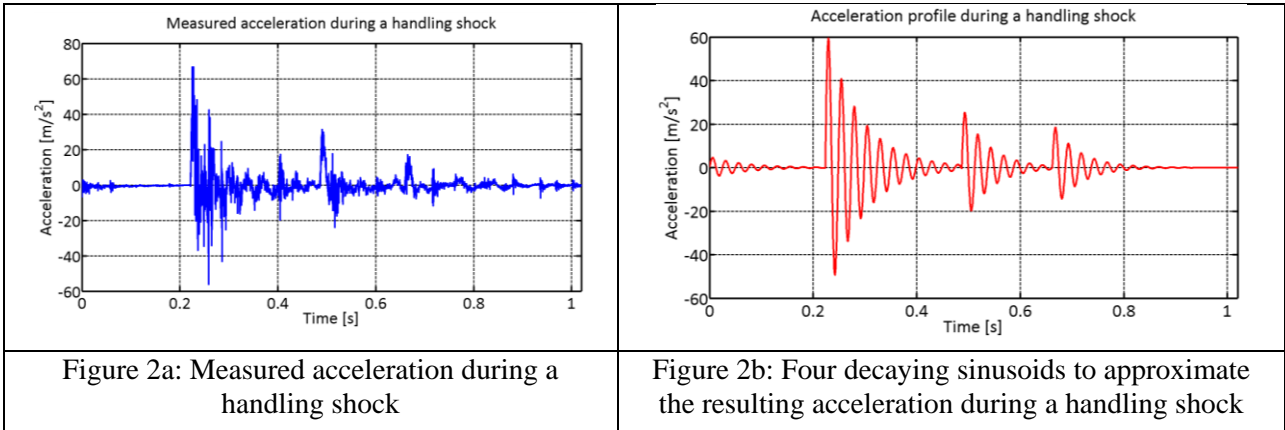
Fragile systems are generally assembled, carried, moved, and transported by trained personnel. Nonetheless, it is hardly possible to completely avoid mechanical excitations when performing these tasks. The drop of tools, collisions with neighbouring parts, etc. might lead to the propagation of large accelerations throughout the system and, in turn, to the damage of very expensive optical components. Clearly, these systems should be isolated from their environment, possibly through weak connections. Additionally, hard stops should be implemented in order to restrain the relative displacements of different parts with respect to each other in order to avoid collisions.

In this context, one may distinguish between vibration and shock excitations. Vibration excitations are characterized by a relatively long duration and a small magnitude as well as randomness, whereas shock excitations have a relatively short duration and large magnitude (see also [2]). Both excitation types have to be taken into account while designing robust optomechanical systems that can withstand the resulting loads. Therefore, the possible sources and characteristics of different excitations will be outlined.

With regard to shock excitations, the most obvious corresponding functions are step and pulse functions, whereas with regard to vibration excitations, noisy spectra could be expected. Nevertheless, the better the prescribed mathematical functions match the real excitation functions with regard to the magnitude and the frequency spectrum, the more accurate the theoretical prediction of the dynamic response and the dimensioning of optomechanical systems will be. The determination of appropriate mathematical functions is therefore a key issue. In the next subsections, we revisit some of these load cases to which realistic excitation functions are assigned.

2.1 Handling and Drop Shock

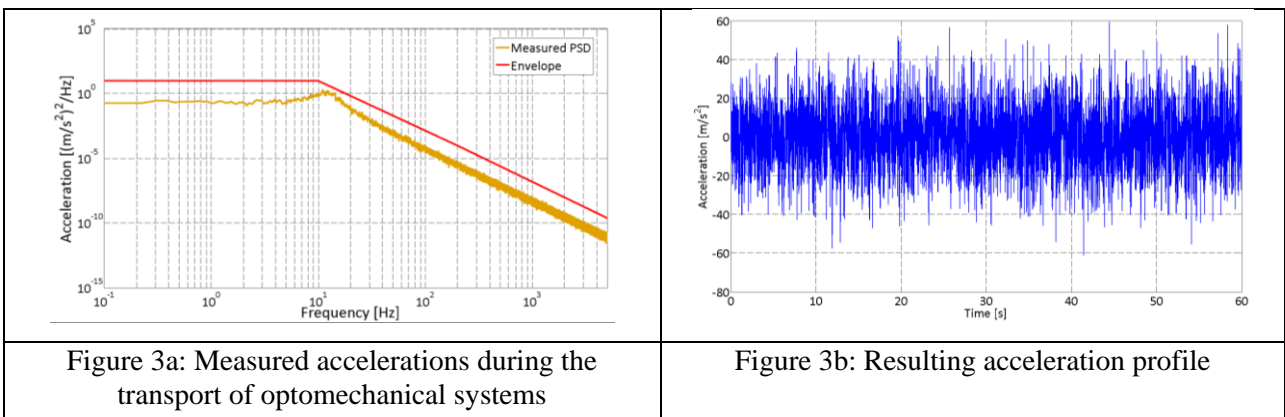
The handling and assembling of optomechanical systems is extremely crucial because optical subsystems are directly exposed to external excitations during these tasks. Figure 2a shows the acceleration measured during a handling shock. Figure 2b shows a profile that is intended to reproduce the measured acceleration. Four decaying sinusoids are used to obtain a profile similar to the measured one.



It should be pointed out that half-sine functions are often used to model shock excitations. In this work, we prefer decaying sinusoids because they are more realistic.

2.2 Transport

Fragile systems such as those under study are usually transported by means of special transport boxes that are intended to dynamically isolate these systems from their vibrating environment. These boxes help to reduce the magnitude of high-frequency vibrations. Owing to the randomness of these excitations, they are better characterized by the representation of their power spectrum density (PSD). As shown in Figure 3a, the typical PSD of these vibrations might have a slope of up to -40 dB/decade once the last rigid body frequency of the transport box is passed. This is mainly because of the connection of the optomechanical system to the transport box, which can be considered as a low-pass filter. Figure 3b shows an acceleration profile, the PSD of which corresponds to that shown in Figure 3a.



Once external excitations can be characterized by mathematical functions, a multi-body model of the optomechanical system with hard stops will help to determine the quantities needed for a robust design.

3 Simplified Modelling of Optomechanical Systems

As mentioned above, fragile optomechanical systems should possess weak connections and hard stops. The former ensures that the magnitude of high-frequency vibrations is reduced, and the latter, that the relative displacements between the optical elements are restricted. The study of such systems should therefore account for the non-linear behaviour due to hard stops that exert discontinuous forces on the optical elements. A linear model, however, could be numerically more efficient to perform parameter variations and derive stiffness and damping specifications. The next generic example points out the challenges related to these issues. In this section, the numerical values of the quantities to be considered are not reported. We rather focus on qualitative investigations.

3.1 Generic Example of an Optomechanical System with Hard Stops

Without loss of generality, we consider a base-excited mass-spring system (see Figure 4). Apart from damped soft mounts, that is, linear springs and viscous dampers, that connect n optical elements (either reflecting surfaces or lenses), hard stops are used to ensure that the relative displacements, and, in turn, the relative forces, between the optical elements remain limited. As mentioned above, these hard stops are required whenever large displacements are expected; the springs yield a low-pass behaviour that is needed to dynamically decouple the optical elements from the rest of the machine. It should be noted that low-pass behaviour alone is not sufficient to prevent collisions.

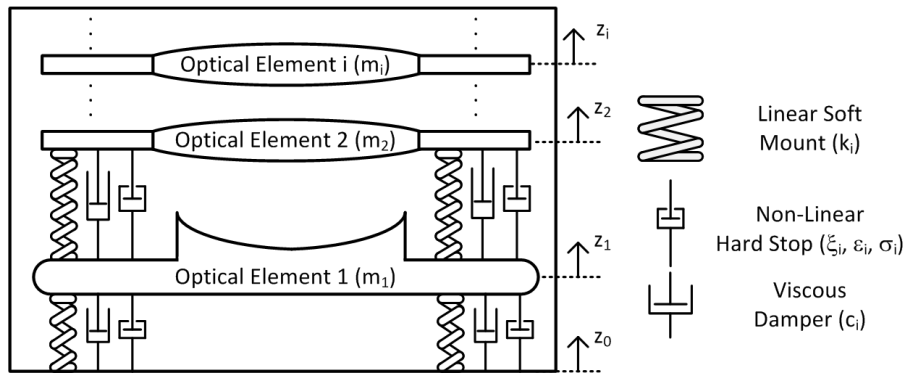


Figure 4: Schematic representation of a generic base-excited optomechanical system

The equation of motion of the i -th optical element reads as follows:

$$m_i \ddot{z}_i + (k_i + |\sigma_i| \xi_i + k_{i+1} + |\sigma_{i+1}| \xi_{i+1}) z_i - (k_{i+1} + |\sigma_{i+1}| \xi_{i+1}) z_{i+1} - (k_i + |\sigma_i| \xi_i) z_{i-1} = \sigma_i \xi_i \varepsilon_i + \sigma_{i+1} \xi_{i+1} \varepsilon_{i+1}, \quad (1)$$

where k_i is the stiffness of the spring connecting masses m_i and m_{i+1} ; ξ_i , the stiffness of the hard stop acting between the aforementioned masses; and ε_i , the gap in the hard stops, that is, the distance that can be travelled before the hard stops are active. σ_i denotes whether the i -th hard stop is active. The mathematical function associated with this constraint could be formulated as follows:

$$\sigma_i = \begin{cases} 0, & \text{if } |z_i - z_{i-1}| \leq \varepsilon_i \\ 1, & \text{if } z_i - z_{i-1} > \varepsilon_i \\ -1, & \text{if } z_i - z_{i-1} < -\varepsilon_i \end{cases} \quad (2)$$

For the first mass ($i = 1$), z_0 has to be derived from the excitations, introduced in Section 3. For the last mass ($i = n$), all parameters related to the (non-existing) optical element with the index $i + 1$ are zero. The term on the right-hand side of Eq. (1) is a correction term which comes into account if the gap ε_i in the hard stop is exceeded. Indeed, along the gap, the hard stops are not active. For simplicity of exposition,

the damping terms were not considered in Eq. (1). Their formulation is, however, very similar to that of the stiffness terms.

Furthermore, it should be noted that a smoother function for σ_i could be chosen in order to make the numerical solving of the differential equations more efficient.

The resulting equation of motion does not differ from the well-known equation:

$$\mathbf{M}\ddot{\mathbf{z}}(t) + \mathbf{C}\dot{\mathbf{z}}(t) + \mathbf{Kz}(t) = \mathbf{u}(t), \quad (3)$$

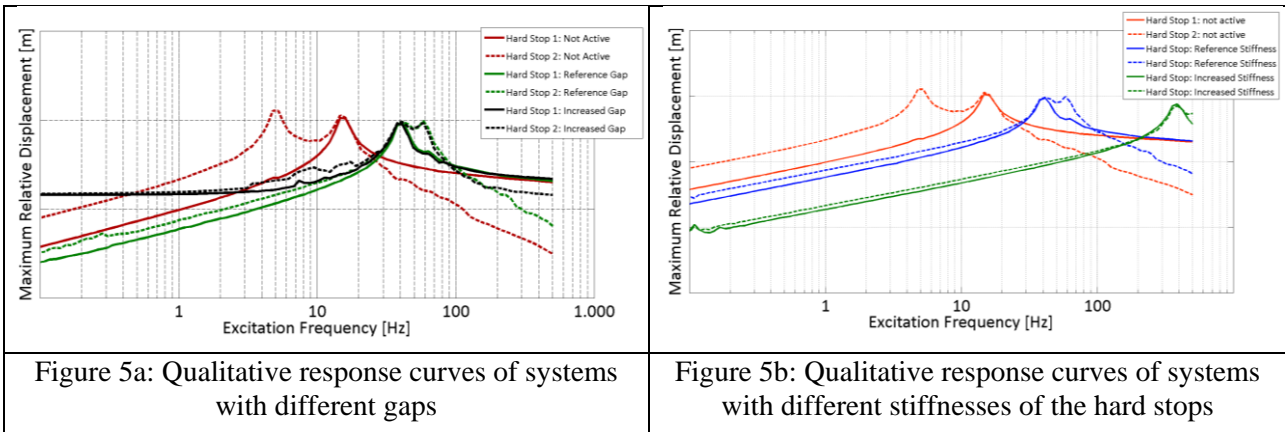
where \mathbf{M} is the mass matrix; \mathbf{z} is the vector containing the absolute displacements of the masses; and \mathbf{u} is the excitation vector whose first component contains the base-excitation function $z_0(t)$. \mathbf{K} and \mathbf{C} are, respectively, the stiffness and damping matrixes. Apart from the stiffness and damping of the springs, they also include the hard stops' stiffness and damping. Hence, the dynamic response of this non-linear system will be significantly affected by the hard stops.

At the end of this section, it should be noted that complex optomechanical systems may be implemented within a multi-body software. Nevertheless, analytical models allow for a better understanding of the dynamic behaviour. The most adequate approach might be to begin with simple analytical equations and then proceed with the implementation of more complex 3D multi-body models. The main task now is to compute the dynamic response of this simplified system in terms of relative displacements. This quantity is the most relevant one in this context because it is a measure of the relative forces as well as of the stress in both the optical elements and the hard stops. Moreover, it is an indicator of collision.

3.2 Dynamic Response to Different Excitations

In this section, we are mainly concerned with the dynamic response of the optomechanical system presented in the previous section. For this purpose, the system is excited by sine functions with different amplitudes and frequencies. The qualitative dynamic response in terms of maximum relative displacement, that is, $|z_{i+1} - z_i|$, between the optical elements is shown in Figure 5. These diagrams are obtained by computing the transient response and taking the maximum value for each excitation frequency. This representation can be considered a measure of the sensitivity of the optomechanical system to shock or vibration excitations. Hence, it allows for the characterization of its robustness.

If the hard stops are not active, the system is linear. Correspondingly, it exhibits two generic resonance frequencies at 5 and 15 Hz. The system's response vanishes at low frequencies and levels off towards high frequencies for the first optical element (as is observed for base excitation). If the hard stops are active, the response exhibits peaks at frequencies larger than the natural frequencies of the linear system because of the additional stiffness of the hard stops. This representation also points out that additional hard stops help to decrease the maximum relative displacements between the optical elements in the subcritical region. Figure 5a shows the influence of increasing the gaps. It is noteworthy that a large gap yields major changes in the dynamic behaviour of the system, especially for low frequencies. In contrast to systems with smaller gaps, those with large gaps do not guarantee that relative displacements remain restricted for static excitations because the motion of one excited base or optical element is not transmitted to the next optical element. Figure 5b highlights the advantages of increasing the stiffness of the hard stops that always lead to reducing the relative displacements for a wider range of frequencies. Increasing the amplitude of the excitation function also affects the maximum relative displacements but has no major impact on the curve for given parameters of the hard stops.



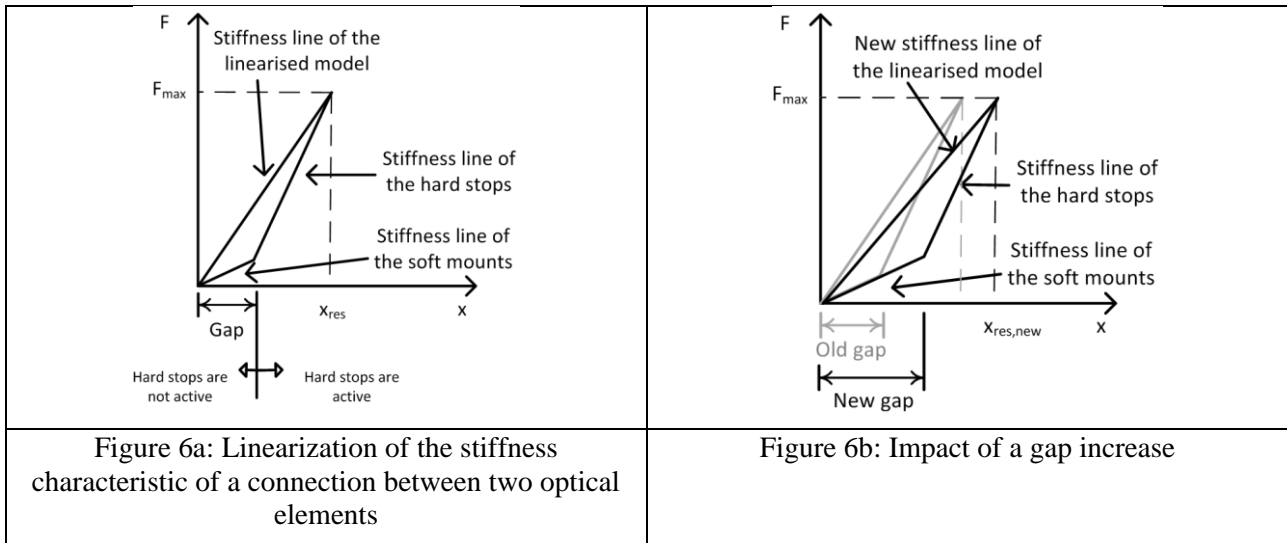
As we are dealing with non-linear systems, it is questionable whether the response of systems possessing hard stops can be deduced from the results of harmonic excitations. For this reason, the excitations discussed above are applied to systems with different parameters. It turns out that the conclusions drawn in this section are valid for a wide spectrum of excitations, with some precautions.

Once the dynamic behaviour for different excitation frequencies is known, it is more straightforward to develop design rules for the implementation of hard stops. A reduction of the relative displacements, as well as the risk of collision, between the optical elements may be achieved by using stiff hard stops. In this case, low-frequency excitations are best suppressed. This may be particularly promising, as the largest amplitudes of the excitations discussed above are expected at low frequencies. It should be noted, however, that except for the first optical element, which is directly in contact with the base, high-frequency excitations may also be suppressed for the remaining optical elements. This is mainly because the absolute motion, that is, with respect to a fixed coordinate system, of the first optical element is not observed for high frequencies. The gap should be chosen by focusing on two criteria: it should be small enough to guarantee that the relative displacements remain restricted and large enough so that sudden contact between the optical elements during operation is prevented.

3.3 Linearization for Design Purposes

For design purposes, it is more adequate to deal with linear models since they are more efficient from a computational point of view. Additionally, optimization tasks and parameter variations can be performed more easily based on linear systems. A possible way to do so involves linearizing the overall stiffness line of each connection of the generic optomechanical system presented in the previous section. Figure 6 depicts the stiffness lines of one connection shown in Figure 4. The proposed approach involves using one linear stiffness curve that takes into account the stiffness of the soft mount and that of the hard stop.

Figure 6b points out that an increase in the gap in the hard stops leads to weakening of the connection between optical elements for low frequencies, as seen in Figure 5a. Increasing the stiffness of the hard stops will lead to a higher stiffness of the whole connection. This is also in line with Figure 5b. In this way, we can account for two major effects that are expected of the non-linear system in Section 3.1.



Once the connection stiffness is linearized, it is possible to define an equivalent linear model as shown in Figure 7.

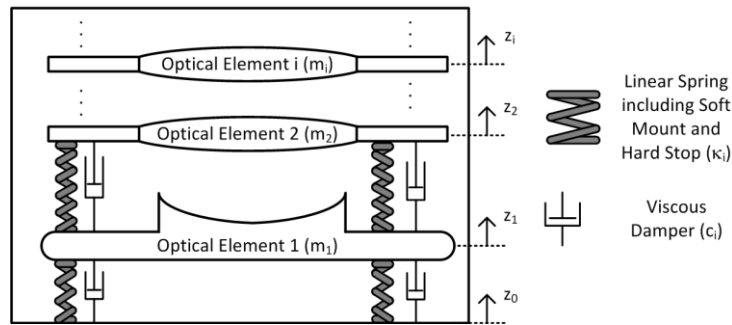


Figure 7: Equivalent linear model

The equation of motion of the *i*-th optical element reads as follows:

$$m_i \ddot{z}_i + (c_i + c_{i+1}) \dot{z}_i + (\kappa_i + \kappa_{i+1}) z_i - c_{i+1} \dot{z}_{i+1} - \kappa_{i+1} z_{i+1} - c_i \dot{z}_{i-1} - \kappa_i z_{i-1} = 0, \quad (4)$$

where κ_i and c_i are, respectively, the stiffness and damping of the connection between optical element *i* and *i* + 1. In contrast to Eq. (1), the equation derived in this section is linear. Hence, its Laplace transformation, as well as the transfer functions $H_i = \frac{Z_i}{Z_0}$, can be calculated. Based on these transfer functions, the relative displacements between all optical elements can be determined in terms of the excitation function $z_0(t)$. When harmonic excitation functions with different frequencies are used, the shock response spectra (see [2]) of Figure 8 are obtained. In addition to estimating the maximum relative displacement of each optical element with respect to the neighbouring one, it is possible to observe the impact of increasing the stiffness and damping of the connections between the optical elements. These curves do not differ much from those shown in Figure 5 despite the linearization.

The proposed approach involves generating for each optical element a shock response spectrum similar to those shown in Figure 8. Based on these diagrams and the frequency content of the expected excitations, rough estimations of the required stiffness and damping can be made for each connection between two different optical elements. In this way, specifications for each connection can be derived. Noting that the expected excitations will not excite all frequencies to the same extent, the system's response near resonances will not necessarily be the most relevant. Moreover, thorough investigations show that elastomer materials are the most adequate for restricting relative displacements and avoiding collisions between optical elements owing to their high damping characteristics.

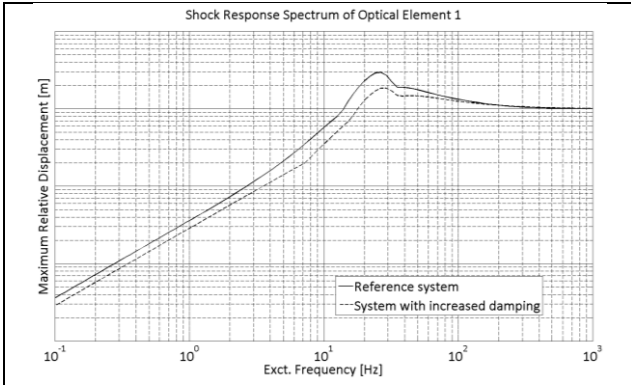


Figure 8a: Influence of damping on the shock response spectrum of optical element 1

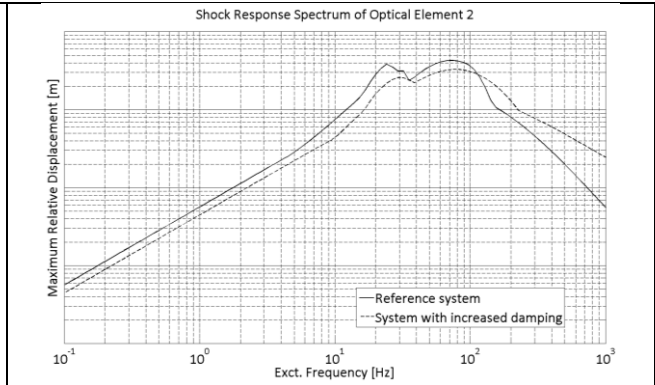


Figure 8b: Influence of damping on the shock response spectrum of optical element 2

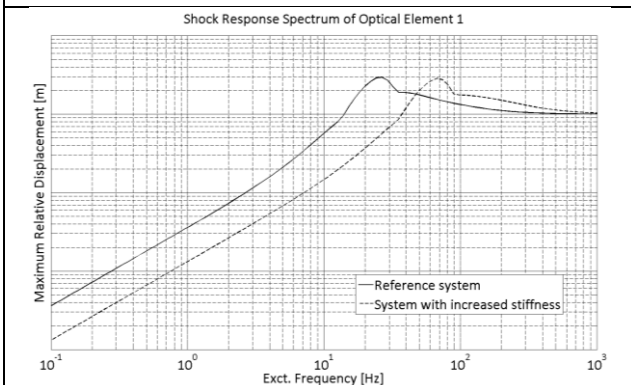


Figure 8c: Influence of increased stiffness on the shock response spectrum of optical element 1

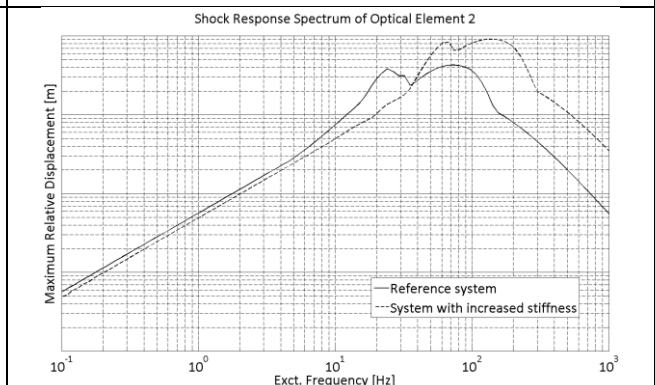


Figure 8d: Influence of increased stiffness on the shock response spectrum of optical element 2

In this section, we showed how one could rely on shock spectra of a linear model to determine the specifications needed for the design of hard stops. The next step involves verifying whether the designed hard stops match the specified stiffness and damping values. First, the design should be verified using an FEA model of one single hard stop that accounts for the non-linear material properties of elastomers. If the results are promising, a prototype can be built. Measurements can then help to identify the dynamic characteristics of the designed hard stop. The next section outlines a possible identification approach.

4 Measurements and Modelling of Hard Stops

In this section, a rheological model is used for the identification of stiffness, viscous damping, and possible friction of one single hard stop mainly made of elastomer material. Figure 9 shows a rheological model consisting of one non-linear spring K^0 and three or more (m) Maxwell elements that, in turn, consist of a linear spring and a viscous damper. In this work, we use Maxwell elements to generate a viscoelastic (frequency-dependent) behaviour and the non-linear spring K^0 to generate an amplitude-dependent behaviour. Generally, Jenkin elements consisting of a linear spring and a frictional element can be used to model amplitude-dependent Coulomb friction. Compared to the use of a non-linear spring, the use of Jenkin elements is more expensive for solving the underlying mathematical equations. Therefore, they are not considered within this work. The resulting relationship between F and u reads as follows:

$$G(u, j\omega) = \frac{F}{u} = K^0(u) + \sum_{i=1}^m \frac{j\omega c_i K_v^i}{j\omega c_i + 1}, \tag{5}$$

where F and u are the displacement and force acting on one hard stop. $K^0(u)$ can be interpreted as the non-linear quasi-static stiffness of the hard stop. ω is the excitation frequency, and c_i and K_v^i are the viscous damping and the (dynamic) stiffness of each Maxwell element, respectively.

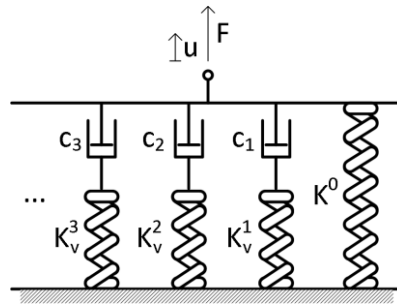


Figure 9: Rheological model of one single hard stop made of elastomer material

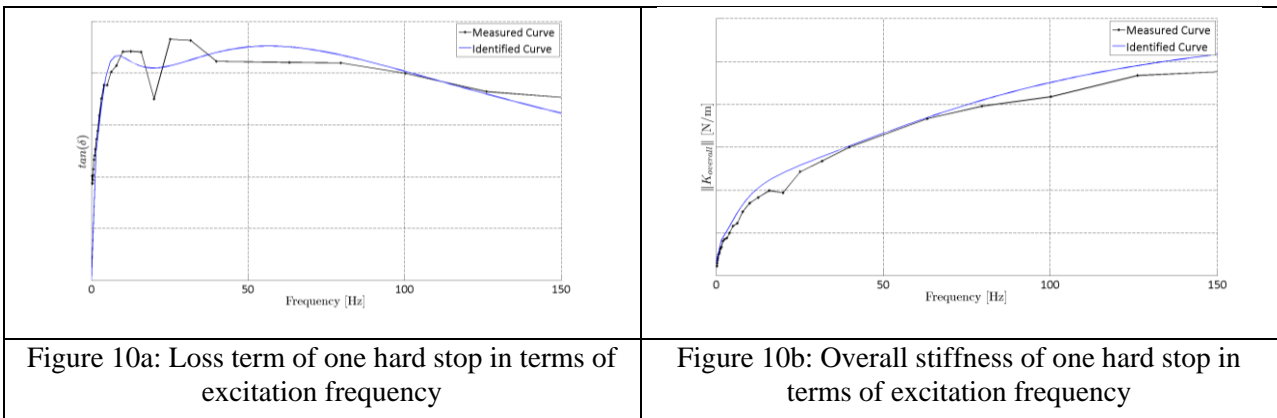
Clearly, the transfer function $G(u, j\omega)$ of Eq. (5) depends on the excitation frequency and the displacement of one hard stop. The overall stiffness $K_{overall}$ of the hard stop is obtained by taking the norm of $G(u, j\omega)$ according to this equation:

$$K_{overall}(u, j\omega) = |G(u, j\omega)|. \tag{6}$$

The overall loss term, $\tan \delta$, can be expressed by

$$\tan \delta = \frac{\text{Im}(G(u, j\omega))}{\text{Re}(G(u, j\omega))}. \tag{7}$$

The overall stiffness and the loss term of Eq. (6) and (7) are usually the measured quantities in this context. The identification task now involves varying the parameters introduced in Eq. (5) to obtain the measured characteristics. Figure 10 shows a possible result of this process.



Based on the results presented in Figure 10, it is possible to compute the reaction force of one hard stop in terms of excitation frequency and displacement. For verification purposes, the model of one single hard stop in Figure 11 can be implemented within the 3D multi-body model of the entire mechanical system to ensure that the real design does not violate any specification.

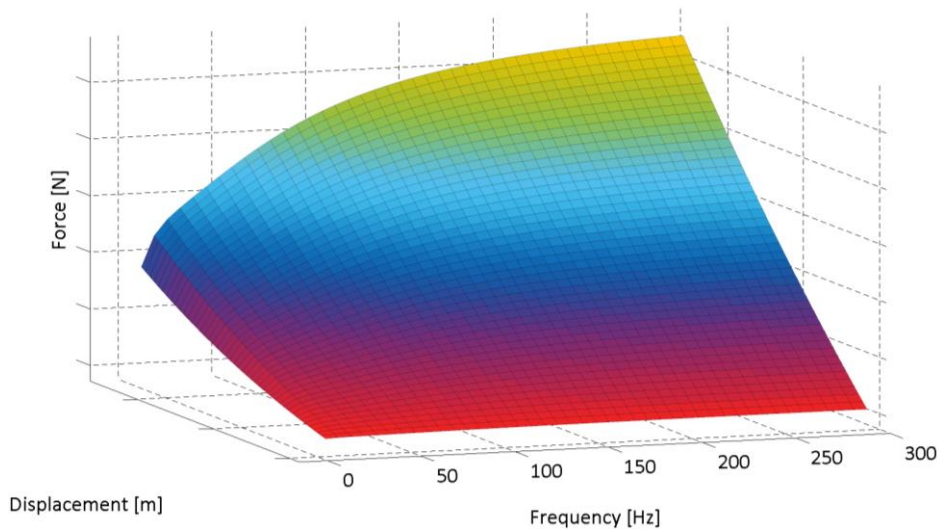


Figure 11: Frequency- and amplitude-dependent force of one hard stop

5 Conclusion

In this work, we focused on excitations that may occur when the machine is out of operation. First, we discussed different shock and vibration excitations in both the time and frequency domains and specified realistic profiles that reflect handling and transport conditions. Using a simplified optomechanical multi-body model, we showed that hard stops are needed in order to ensure that all parts of the system do not collide when they are subject to dynamic excitations. These hard stops create a non-linear system since they exert forces once a predefined range is exceeded. However, we showed that it is possible, to a certain extent, to rely on a linear model at an early stage of the design process. Indeed, this model is more adequate for deriving specifications. We also showed that a rheological model may be used to identify the dynamic characteristics of hard stops made of elastomer materials. The obtained model can be implemented within a multi-body software to validate the final design of the whole optomechanical system. Future works will be devoted to a better FEA modelling of elastomer materials over a wide frequency range in order to reduce the measurement efforts and to simplify the design process.

References

- [1] N. Wengert, M. Nefzi, P. Eberhard, B. Geuppert, *Dynamics in lithographic projection objectives*, *Multibody System Dynamics*, Vol. 30, No. 2, Springer (2013), pp. 233-245.
- [2] A. Piersol, T. Paez, *Harris' Shock and Vibration Handbook*, 6th ed., McGraw-Hill, New York (2009).

